Adaptive backstepping for switching control active magnetic bearing system with vibrating base

S. Sivrioglu

Abstract: This research aims to test the limits of control effectiveness for an active magnetic bearing (AMB) system subjected to external acceleration disturbances. An adaptive output backstepping controller is designed to compute nonlinear control currents of the magnetic bearing by accepting that the rotor and AMB parameters are unknown. The control currents of the electromagnets of the active magnetic bearing is switched according to the rotor position. The adaptive backstepping controller is experimentally verified in an AMB test system with vibrating base and the results are compared with proportional integrative derivative (PID) control results for the maximum amplitude of applicable disturbance.

1 Introduction

An active magnetic bearing (AMB) provides contact-free suspension of a rotor; thus, friction is not present and lubrication is not needed [1, 2]. Therefore the lifetime of an AMB outperforms that of a mechanical bearing. These characteristics make AMBs attractive for many applications especially flywheel energy storage systems. Despite such advantages, the stiffness of a magnetic bearing is low compared with a mechanical bearing.

The safe operation of flywheels should be maintained for any condition. Since flywheels are rotating parts with large kinetic energy capacity depending on the size, they have destructive potential and may cause deadly damages if some failure occurs at high-speed spinning. For large scale flywheel applications, earthquake like disturbances may cause some failures in control systems. Therefore the designed controller should be tested for such kind of disturbances.

Nonlinear control of the active magnetic bearings has been previously studied using different approaches. In [3], a nonlinear control approach is proposed using differential flatness. Input–output linearisation and sliding mode control are applied to AMB systems in [4–6]. As a control design approach, the nonlinear integrator backstepping is propsed to solve control problems for AMB applications [7]. To reduce power losses, low-bias and zero-bias controls of AMBs are studied in [8–11]. In this study, an adaptive output feedback type backstepping control is presented to achieve better performance in the case of acceleration disturbances.

© The Institution of Engineering and Technology 2007

doi:10.1049/iet-cta:20050473

Paper first received 21st November 2005 and in revised form 7th September 2006

The author is with the Faculty of Engineering, Gebze Institute of Technology, Gebze-Turkey

E-mail: s.selim@gyte.edu.tr

2 Problem statement

Consider the vertically designed AMB system depicted in Fig. 1. In this setup, the AMB system is placed on a vibrating base which is connected to a shaker for acceleration disturbance. The flywheel system uses in general three AMBs to suspend the rotor, that is two magnetic actuators in radial direction and one in axial direction. However, the axial bearing is not considered in the following control design unless otherwise stated. Fig. 2 illustrates the flywheel-rotor and placement of the radial magnetic actuators in upper and lower locations in xGz plane. The parameters of the flywheel AMB system is given in Table 1. Note that four other magnetic actuators are also placed in yGz plane symmetrically, but are not shown in Fig. 2.

In most AMB systems, the controller is designed for normal operating conditions to reduce cost and controller complexity. Besides stability of the system, performance measures are also taken into consideration in normal conditions. But in emergency cases, it is desired that AMB control system must maintain the stability first. Therefore the objective of the control is to provide the stability of the AMB system under the applicable maximum amplitude of acceleration disturbances.

The nonlinear control defined here serves to switch the control current of the electromagnets of the AMB according to the rotor position. Unlike the linear control, no bias current is employed in the proposed nonlinear control. In an attractive type bearing configuration of a pair magnet, when the rotor approaches one of the magnets, the coil current in that magnet switches to zero, whereas the coil current in the magnet on the opposite side is switched on to generate attractive force. The switching process continues until the rotor is brought to the origin and stabilised.

The mathematical model of the flywheel AMB system is derived and the upper and lower AMB equations are separated each other by using some assumption (see the Appendix). After this process, each axis of the AMB becomes independent of each other. The structure of the nonlinear switching control may be defined only for one axis.

Authorized licensed use limited to: FUDAN UNIVERSITY. Downloaded on February 17,2010 at 15:49:13 EST from IEEE Xplore. Restrictions apply.

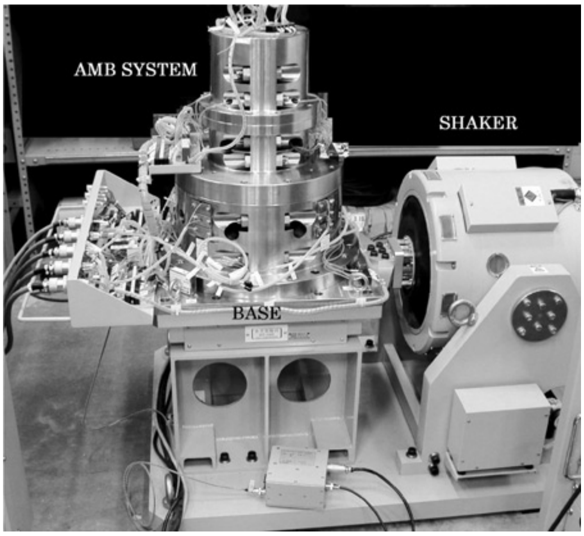

Fig. 1 *Photo of the AMB system*

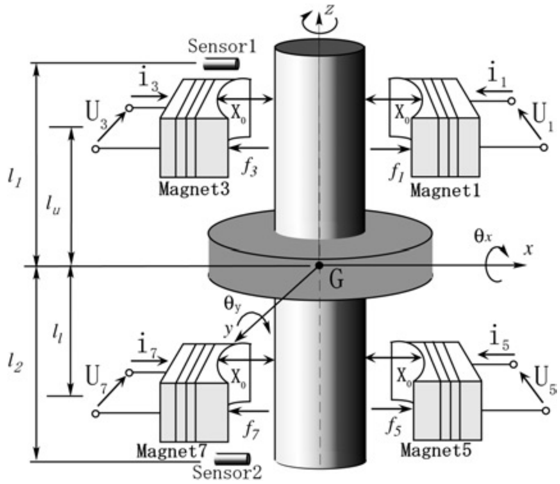

Fig. 2 *Flywheel rotor-AMB system*

Using the variable transformations $x_1 = x_u$ and $x_2 = \dot{x}_u$ in (29), the second-order system is obtained as

$$\begin{aligned} \dot{x}_1 &= x_2 \\ \dot{x}_2 &= \begin{bmatrix} \theta\beta_1(x_1) & -\theta\beta_3(x_1) \end{bmatrix} \begin{bmatrix} u_1 \\ u_3 \end{bmatrix} \\ y &= x_1 \end{aligned} \tag{1}$$

where $u_1 = i_1^2$ and $u_3 = i_3^2$ are the control inputs. y denotes the output of the system. The unknown parameter θ and the nonlinear functions β_1 and β_3 are defined as

$$\begin{gathered} \theta = a_u K_u \\ \beta_1(x_1) = \frac{1}{(X_0 - x_1)^2}, \quad \beta_3(x_1) = \frac{1}{(X_0 + x_1)^2} \end{gathered} \tag{2}$$

Note that the nonlinear functions β_1 and β_3 are strictly positive functions of the state x_1. It seems that (1) has multiple inputs but in reality only one control input is effective at any time depending on the rotor position. If (1) is rearranged as

$$\begin{aligned} \dot{x}_1 &= x_2 \\ \dot{x}_2 &= \theta\beta u \\ y &= x_1 \end{aligned} \tag{3}$$

The following switching rule is necessary to realise the proposed control structure

$$\begin{array}{llll} \text{if } x_1 \geq 0 & u = u_3, & u_1 = 0, & \beta = -\beta_3(x_1) \\ \text{if } x_1 < 0 & u = u_1, & u_3 = 0, & \beta = \beta_1(x_1) \end{array} \tag{4}$$

3 Adaptive output backstepping

3.1 Nonlinear observer

In practice, only the displacement of the rotor is measured using position sensors, and the velocity is not available for the feedback. To estimate the unmeasured state x_2, an exponentially convergent observer is introduced into the control system such as

$$\hat{x}_2 = \eta + \theta\lambda + kx_1 \tag{5}$$

where η and λ denote the states of the filters. Also, k is a positive parameter. The first filter is for the part of the plant that does not contain the unknown parameter θ and the second one is for the unknown part of the plant. The filters are defined as

$$\begin{aligned} \dot{\eta} &= -k\eta - k^2 x_1 \\ \dot{\lambda} &= -k\lambda + \beta(x_1)u \end{aligned} \tag{6}$$

If the initial conditions are $\eta(0) = 0$ and $\lambda(0) = 0$, then it is guaranteed that the estimation error ϵ exponentially

Table 1: Parameters of the AMB system

Symbol	Meaning	Value	Unit
M	mass of the rotor	10.78	kg
I_r	moment of inertia	0.150573	kgm^2
I_a	polar moment of inertia	0.0275912	kgm^2
l_u	distance of upper AMB from the centre of mass	0.22467	m
l_l	distance of lower AMB from the centre of mass	0.13033	m
l_1	distance of the upper sensor from the centre of mass	0.26817	m
l_2	distance of the lower sensor from the center of mass	0.17409	m
K	Magnetic bearing coefficient	2.463×10^{-7}	Nm^2/A^2
X_0, Y_0	gap between the rotor and AMB	0.5×10^{-3}	m
K_s	Sensor gain	10 000	V/m

Authorized licensed use limited to: FUDAN UNIVERSITY. Downloaded on February 17,2010 at 15:49:13 EST from IEEE Xplore. Restrictions apply.

converges to zero

$$
\begin{aligned}
\epsilon &= x_2 - \hat{x}_2 \\
\dot{\epsilon} &= \dot{x}_2 - \dot{\eta} - \theta\dot{\lambda} - k\dot{x}_1 \\
&= k(\eta + \theta\lambda + kx_1) - kx_2 \\
&= -k\epsilon
\end{aligned}
\tag{7}
$$

3.2 Control design

The adaptive backstepping controller will be designed in detail as defined in [12]. The error between measured rotor displacement and the reference $y_r(t)$ is defined as

$$
z_1 = y - y_r \tag{8}
$$

The derivative of z_1 is obtained as

$$
\begin{aligned}
\dot{z}_1 &= \dot{x}_1 - \dot{y}_r \\
&= x_2 - \dot{y}_r
\end{aligned}
\tag{9}
$$

Since x_2 is not measured, the estimate of it will be used. Now substituting (5) into (9), the derivative of z_1 becomes

$$
\dot{z}_1 = \eta + \theta\lambda + kx_1 + \epsilon \tag{10}
$$

Note that the reference input y_r is zero for the rotor magnetic bearing system. The aim of the control here is to bring the rotor to the origin or zero axes. Therefore, to force the error to zero means to force the rotor to the origin. In (10), the only variable that contains control input u is λ. Thus, λ may be used to define the second error variable such as

$$
z_2 = \lambda - \alpha_1 \tag{11}
$$

where α_1 is a stabilising function and is chosen as

$$
\alpha_1 = \hat{\rho}\,(-c_1 z_1 - d_1 z_1 - kx_1 - \eta) = \hat{\rho}\bar{\alpha}_1 \tag{12}
$$

where $c_1 > 0$, $d_1 > 0$. Note that to eliminate λ in (10), the stabilising function α_1 is multiplied by $\hat{\rho}$ which is an estimate of the parameter $\rho = 1/\theta$. Moreover, unlike in the integrator backstepping procedure, d_1 is added to counteract the estimation error ϵ. Now, the derivative of z_1 becomes

$$
\begin{aligned}
\dot{z}_1 &= \eta + \theta(z_2 + \alpha_1) + kx_1 + \epsilon \\
&= \eta + \theta[z_2 + (\rho - \tilde{\rho})\bar{\alpha}_1] + kx_1 + \epsilon \\
&= \theta z_2 - c_1 z_1 - d_1 z_1 - \theta\tilde{\rho}\bar{\alpha}_1 + \epsilon
\end{aligned}
\tag{13}
$$

where $\hat{\rho} = \rho - \tilde{\rho}$. Here, $\tilde{\rho}$ denotes the error in the estimation of $\hat{\rho}$. A candidate Lyapunov function for the first error variable is defined as

$$
V_1 = \frac{1}{2}z_1^2 + \frac{1}{2\gamma}\theta(\rho - \hat{\rho})^2 + \frac{1}{2kd_1}\epsilon^2 \tag{14}
$$

where γ is the adaptation gain. The derivative of V_1 is obtained as

$$
\begin{aligned}
\dot{V}_1 &= z_1\dot{z}_1 - \frac{1}{\gamma}\theta(\rho - \hat{\rho})\dot{\hat{\rho}} + \frac{1}{kd_1}\epsilon\dot{\epsilon} \\
&= \theta z_1 z_2 - c_1 z_1^2 - \theta(\rho - \hat{\rho})\left(\bar{\alpha}_1 z_1 + \frac{1}{\gamma}\dot{\hat{\rho}}\right) \\
&\quad \underbrace{-\,d_1\left(z_1 - \frac{1}{2d_1}\epsilon\right)^2 + \frac{1}{4d_1}\epsilon^2}_{-d_1 z_1^2 + z_1\epsilon} - \frac{1}{d_1}\epsilon^2 \\
&\le \theta z_1 z_2 - c_1 z_1^2 - \theta(\rho - \hat{\rho})\left(\bar{\alpha}_1 z_1 + \frac{1}{\gamma}\dot{\hat{\rho}}\right) - \frac{3}{4d_1}\epsilon^2
\end{aligned}
\tag{15}
$$

The $\theta(\rho - \hat{\rho})$ term in the above inequality can be eliminated using the update law as follows

$$
\dot{\hat{\rho}} = -\gamma\bar{\alpha}_1 z_1 \tag{16}
$$

Since the term $\theta z_1 z_2$ remained in (15), a global stability condition is not satisfied in this step. The second step is to expand the control design to include the error variable z_2. To this aim, the derivative of the second error variable is given as

$$
\dot{z}_2 = \dot{\lambda} - \dot{\alpha}_1 \tag{17}
$$

Here, the stabilising function α_1 is a function of y, η and $\hat{\rho}$. The derivative of α_1 is obtained as

$$
\dot{\alpha}_1 = \frac{\partial\alpha_1}{\partial y}\dot{y} + \frac{\partial\alpha_1}{\partial\eta}\dot{\eta} + \frac{\partial\alpha_1}{\partial\hat{\rho}}\dot{\hat{\rho}} \tag{18}
$$

Substituting (6) and (18) into (17), the derivative of z_2 becomes

$$
\begin{aligned}
\dot{z}_2 &= -k\lambda + \beta(x_1)u - \frac{\partial\alpha_1}{\partial y}(\eta + \theta\lambda + kx_1 + \epsilon) \\
&\quad - \frac{\partial\alpha_1}{\partial\eta}(-k\eta + k^2 x_1) - \frac{\partial\alpha_1}{\partial\hat{\rho}}\dot{\hat{\rho}}
\end{aligned}
\tag{19}
$$

Equation (19) is not a desired form because the unknown parameter θ appears. Moreover, the disturbance ϵ is multiplied by the nonlinear term $(\partial\alpha_1/\partial y)$. To employ nonlinear damping and to eliminate the unknown parameter, (19) is equalised as follows

$$
\begin{aligned}
&-c_2 z_2 - \hat{\theta}\, z_1 - d_2\left(\frac{\partial\alpha_1}{\partial y}\right)^2 z_2 - \frac{\partial\alpha_1}{\partial y}\epsilon - \frac{\partial\alpha_1}{\partial y}\tilde{\theta}\lambda \\
&= -k\lambda + \beta(x_1)u - \frac{\partial\alpha_1}{\partial y}(\eta + \theta\lambda + kx_1 + \epsilon) \\
&\quad - \frac{\partial\alpha_1}{\partial\eta}(-k\eta - k^2 x_1) - \frac{\partial\alpha_1}{\partial\hat{\rho}}\dot{\hat{\rho}}
\end{aligned}
\tag{20}
$$

where $\hat{\theta}$ is the estimate of the unknown parameter θ. Also, $\tilde{\theta}$ represents error in this estimation. From (20), the control

Authorized licensed use limited to: FUDAN UNIVERSITY. Downloaded on February 17,2010 at 15:49:13 EST from IEEE Xplore. Restrictions apply.

input u is obtained as

$$u = \frac{1}{\beta(x_1)}\left[-c_2 z_2 - d_2\left(\frac{\partial\alpha_1}{\partial y}\right)^2 z_2 - \hat{\theta} z_1 \right.$$
$$+ k\lambda + \frac{\partial\alpha_1}{\partial y}(\eta + \hat{\theta}\lambda + k x_1)$$
$$\left. + \frac{\partial\alpha_1}{\partial\eta}(-k\eta - k^2 x_1) + \frac{\partial\alpha_1}{\partial\hat{\rho}}\dot{\hat{\rho}}\right] \tag{21}$$

Substituting (21) into (19), the derivative of z_2 becomes

$$\dot{z}_2 = -c_2 z_2 - d_2\left(\frac{\partial\alpha_1}{\partial y}\right)^2 z_2 - (\theta - \tilde{\theta}) z_1$$
$$- \frac{\partial\alpha_1}{\partial y}\tilde{\theta}\lambda - \frac{\partial\alpha_1}{\partial y}\epsilon \tag{22}$$

The Lyapunov function is augmented for the second error variable z_2 as follows

$$V_2 = V_1 + \frac{1}{2}z_2^2 + \frac{1}{2\gamma}(\theta - \hat{\theta})^2 + \frac{1}{2kd_2}\epsilon^2 \tag{23}$$

The derivative of V_2 is derived as

$$\dot{V}_2 = \dot{V}_1 + z_2\dot{z}_2 - \frac{1}{\gamma}(\theta - \hat{\theta})\dot{\hat{\theta}} + \frac{1}{kd_2}\epsilon\dot{\epsilon}$$
$$= -c_1 z_1^2 - c_2 z_2^2 - \underbrace{d_2\left(\frac{\partial\alpha_1}{\partial y}z_2 - \frac{1}{2d_2}\epsilon\right)^2 + \frac{1}{4d_2}\epsilon^2}_{d_2(\frac{\partial\alpha_1}{\partial y})^2 z_2^2 - \frac{\partial\alpha_1}{\partial y}\epsilon z_2}$$
$$- \frac{1}{d_2}\epsilon^2 - \frac{3}{4d_1}\epsilon^2 \leq -c_1 z_1^2 - c_2 z_2^2 + (\theta - \hat{\theta})$$
$$\times\left(z_1 z_2 - \frac{\partial\alpha_1}{\partial y}\lambda z_2 - \frac{1}{\gamma}\dot{\hat{\theta}}\right) - \left(\frac{3}{4d_1} + \frac{3}{4d_2}\right)\epsilon^2 \tag{24}$$

where $c_2 > 0$, $d_2 > 0$. The unknown part of $(\theta - \hat{\theta})$ in (24) is eliminated using the update law

$$\dot{\hat{\theta}} = \gamma\left(z_1 z_2 - \frac{\partial\alpha_1}{\partial y}\lambda z_2\right) \tag{25}$$

It is clear that a global stability is maintained in the final Lyapunov function. The control currents i_1 and i_3 can be computed from the control input u obtained in (21).

4 Experiments

A feedback control system is built using a high-speed Texas instrument digital signal processor (TMS320C6701) to realise experiments. The control system is a multi-input multi-output structure with four displacements measured by four eddy current position sensors and eight computed control current signals for actuators. The control inputs are supplied to electromagnets through D/A converters and power amplifiers.

In rotor-AMB systems, trajectories of the geometric centre point of the rotor and control currents are generally used to evaluate the control performance. Since the limits of the control effectiveness are aimed, the base is subjected to acceleration disturbance at a fixed frequency of 10 Hz but the amplitude of the disturbance is continuously increased up to the touch down position of the rotor. Note that the AMB setup is placed on the base to make 45° of angle with the axis of actuators so that the disturbance effect is equally distributed both x and y directions. The results are obtained for the maximum amplitude of the disturbance. In this study, the results of lower actuator location are presented because the disturbance effect is large compared to upper AMB location.

The flywheel AMB system is rotated up to 60 Hz and acceleration disturbance is applied to the base at 50 Hz. Figs. 3 and 4 show the displacement and orbits of the rotor for backstepping adaptive control case ($\omega = 50$), respectively. The control currents of the lower actuator are presented in Fig. 5. The control current characteristics reflect the proposed nonlinear switching control principle clearly. From Figs. 6–8, the PID control results are presented for the same location of the actuator. For comparison of both cases, the maximum applied acceleration disturbance is shown in Fig. 9. As seen in this figure, the adaptive control maintains the stability of AMB system even the amplitude of disturbance approximately two times higher than PID control case. The control currents are almost same level for both case. Note that PID is a linear controller and a 0.5 A bias current is applied to the magnetic actuators in PID control.

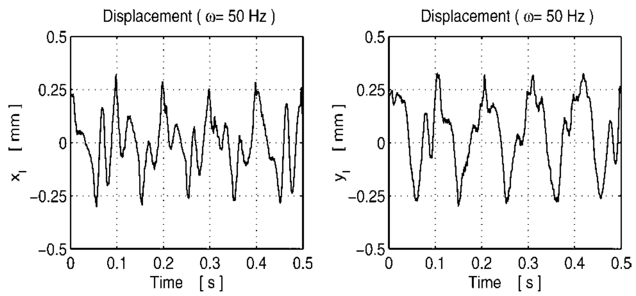

Fig. 3 *Displacement of the rotor (adaptive control)*

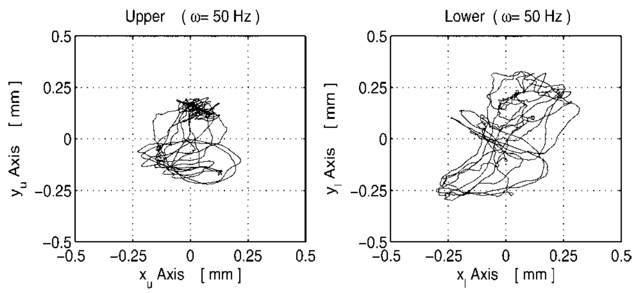

Fig. 4 *Orbit of the rotor (adaptive control)*

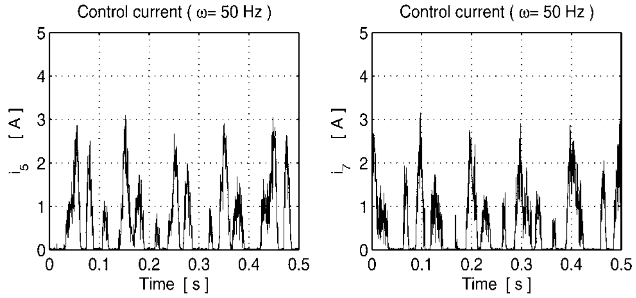

Fig. 5 *Control currents (adaptive control)*

Authorized licensed use limited to: FUDAN UNIVERSITY. Downloaded on February 17,2010 at 15:49:13 EST from IEEE Xplore. Restrictions apply.

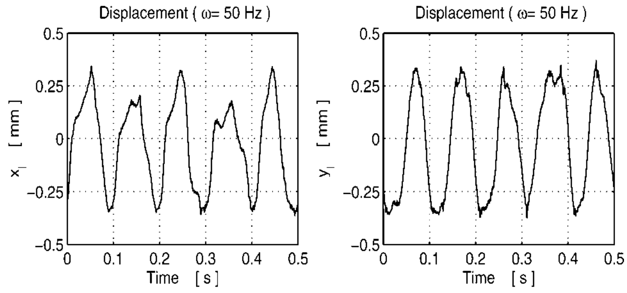

Fig. 6 *Displacement of the rotor (PID control)*

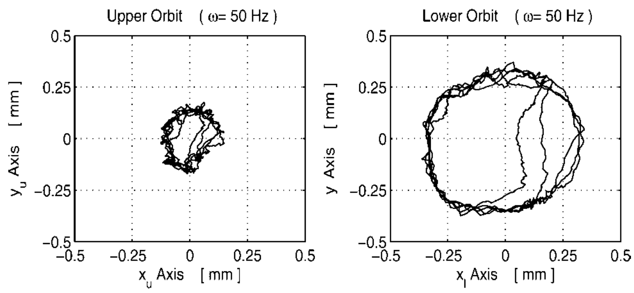

Fig. 7 *Orbit of the rotor (PID control)*

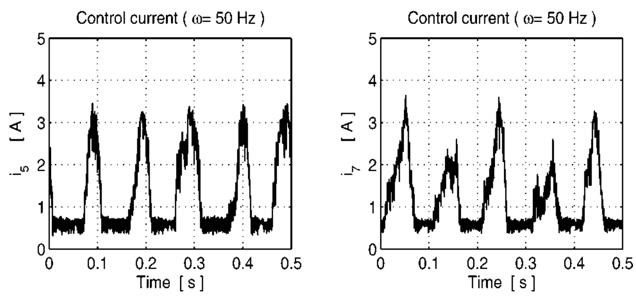

Fig. 8 *Control currents (PID control)*

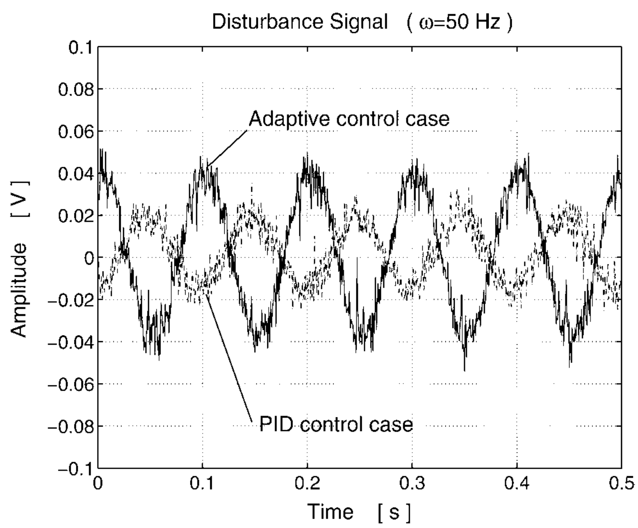

Fig. 9 *Acceleration disturbance*

5 Conclusions

The design of adaptive output backstepping control is presented for a nonlinear switching AMB system. The nonlinear observers are used to provide the estimate of the unmeasured state with an exponentially convergent error decay since the full state of the control system is not available for the feedback. The control systems of AMB setup are tested experimentally with base acceleration disturbance at different rotational speeds. The bearable acceleration disturbance level of adaptive control was two times higher than PID control.

6 References

1 Schweitzer, G., Bleuler, H., and Traxler, A.: 'Active magnetic bearings'. (vdf Hochschuverlag AG an der ETH Zurich, 1994)

2 Schweitzer, G.: 'Active magnetic bearings-chances and limitations'. Proc. of the 6th Int. IFToMM Conf. on Rotor Dynamics, 2002, Sydney, Australia, pp. 1–14

3 Levine, J., Lottin, J., and Ponsart, J-C.: 'A nonlinear approach to the control of magnetic bearing', *IEEE Trans. Control System Technol.*, 1996, **4**, (5), pp. 524–544

4 Chara, A., Miras, J.D., and Caron, B.: 'Nonlinear control of a magnetic levitation system without premagnetization', *IEEE Trans. Control Syst. Technol.*, 1996, **4**, (5), pp. 513–523

5 Smith, R.D., and Weldon, W.F.: 'Nonlinear control of a rigid rotor magnetic bearing system: modeling and simulation with full state feedback', *IEEE Trans. Magn.*, 1995, **31**, (2), pp. 973–980

6 Sivrioglu, S., and Nonami, K.: 'Sliding mode control with time varying hyperplane for AMB systems', *IEEE/ASME Trans. Mechatron.*, 1998, **3**, (1), pp. 51–59

7 Queiroz, M.S., and Dawson, D.M.: 'Nonlinear control of active magnetic bearings: a backstepping appproach', *IEEE Trans. Control Syst. Technol.*, 1996, **4**, (5), pp. 545–552

8 Tsiotras, P., and Arcak, M.: 'Low-bias control of AMB subject to voltage saturation: state-feedback and observer design', *IEEE Trans. Control Syst. Technol.*, 2005, **13**, (2), pp. 262–273

9 Ariga, Y., Nonami, K., and Sakai, K.: 'Nonlinear control of zero power magnetic bearing using Lyapunov's direct method'. Proc. of the 7th ISMB, , pp. 293–298

10 Sivrioglu, S.: 'Adaptive control of nonlinear zero-bias magnetic bearing system', *Nonlinear Dynamics*, 2007, **48**, pp. 175–184

11 Sivrioglu, S., Nonami, K., and Saigo, M.: 'Low power consumption nonlinear control with H-infinity compensator for a zero-bias flywheel AMB system', *J. Vibration Control*, 2004, **10**, (8), pp. 1151–1166

12 Krstic, M., Kanellakopoulos, I., and Kokotovic, P.: 'Nonlinear and adaptive control design' (John Wiley & Sons, Inc, 1995)

7 Appendix

The equation of motion of the rigid rotor AMB system depicted in Fig. 2 is derived as

$$\begin{aligned} M\ddot{x}_g &= f_{xu} + f_{xl} \\ I_r\ddot{\theta}_y &= -I_a\omega\dot{\theta}_x + l_u f_{xu} - l_l f_{xl} \\ M\ddot{y}_g &= f_{yu} + f_{yl} \\ I_r\ddot{\theta}_x &= I_a\omega\dot{\theta}_y - l_u f_{yu} + l_l f_{yl} \end{aligned} \tag{26}$$

where $-I_a\omega\dot{\theta}_x$ and $I_a\omega\dot{\theta}_y$ are gyroscopic terms. Since the polar moment of inertia is small, gyroscopic effects can be ignored in modelling and control design. The control forces are

$$\begin{aligned} f_{xu} &= (f_1 - f_3), \quad f_{xl} = (f_5 - f_7) \\ f_{yu} &= (f_2 - f_4), \quad f_{yl} = (f_6 - f_8) \end{aligned} \tag{27}$$

The equations of motion obtained in (26) are derived according to the movement of the rotor's centre of mass. On the other hand, the measured signals are the displacements of the rotor at the lower and upper sensor locations. Since sensor locations are distinct from the mass centre, the computation of the displacements of the rotor's center of mass and angular displacements are necessary during control operation. Instead of computing the displacements x_g, y_g, θ_y and θ_x, the computation of the displacements of the rotor at the magnet locations makes the control system

Authorized licensed use limited to: FUDAN UNIVERSITY. Downloaded on February 17,2010 at 15:49:13 EST from IEEE Xplore. Restrictions apply.

collocated. To this aim, the equations of the rotor AMB system may be transformed to the actuator locations. The displacement at the upper AMB location for the x direction is obtained as

$$x_u = x_g + l_u \theta_y \tag{28}$$

Taking the double derivative of the above equation and substituting (26) and (27) into the obtained derivations, the equations are derived as

$$\begin{aligned} \ddot{x}_u &= \ddot{x}_g + l_u \ddot{\theta}_y = \frac{1}{M} f_1 - \frac{1}{M} f_3 + l_u \left(\frac{1}{I_r} f_1 l_u - \frac{1}{I_r f_3 l_u} \right) \\ \ddot{x}_u &= a_u \left[\frac{K_u i_1^2}{(X_0 - x_u)^2} - \frac{K_u i_3^2}{(X_0 + x_u)^2} \right] \end{aligned} \tag{29}$$

where

$$a_u = \left(\frac{1}{M} + \frac{l_u^2}{I_r} \right) \tag{30}$$

The transformation of the equations for the location of lower AMB is realised with the same derivation procedure and follows as

$$\begin{aligned} x_l &= x_g - l_l \theta_y \\ \ddot{x}_l &= \ddot{x}_g - l_l \ddot{\theta}_y = \frac{1}{M} f_5 - \frac{1}{M} f_7 - l_l \left(-\frac{1}{I_r} f_5 l_l + \frac{1}{I_r} f_7 l_l \right) \\ \ddot{x}_l &= a_l \left[\frac{K_l i_5^2}{(X_0 - x_l)^2} - \frac{K_l i_7^2}{(X_0 + x_l)^2} \right] \end{aligned} \tag{31}$$

where

$$a_l = \left(\frac{1}{M} + \frac{l_l^2}{I_r} \right) \tag{32}$$

Similarly, the displacement in the y direction is given as

$$\begin{aligned} y_u &= y_g - l_u \theta_x \\ y_l &= y_g + l_l \theta_x \end{aligned} \tag{33}$$

Repeating the same procedure, the transformed equations are derived as

$$\begin{aligned} \ddot{y}_u &= a_u \left[\frac{K_u i_2^2}{(Y_0 - y_u)^2} - \frac{K_u i_4^2}{(Y_0 + y_u)^2} \right] \\ \ddot{y}_l &= a_l \left[\frac{K_l i_6^2}{(Y_0 - y_l)^2} - \frac{K_l i_8^2}{(Y_0 + y_l)^2} \right] \end{aligned} \tag{34}$$

Note that in the above derivation process only the forces that directly effect the considered points are taken into account. When the transformation is done for the upper actuator location (x_u, y_u) on the rotor, the upper AMB forces f_1 and f_3 are considered and f_5, f_7 are taken as zero. For the lower actuator location (x_l, y_l), the forces f_5 and f_7 are assumed to be effective and f_1, f_3 are taken as zero.

Authorized licensed use limited to: FUDAN UNIVERSITY. Downloaded on February 17,2010 at 15:49:13 EST from IEEE Xplore. Restrictions apply.